A diluent protective organic additive electrolyte of hydrophilic hyperbranched polyester for long-life reversible aqueous zinc manganese oxide batteries

Hengxin Xu[1], Song Yang[1], Yufeng Chen[1], Junle Xiong[2], Shengtao Zhang[1], Fang Gao (✉)[1], Zhengyong Huang (✉)[1,3], and Hongru Li (✉)[1]

1 College of Chemistry and Chemical Engineering, Chongqing University, Chongqing 400044, China
2 Chongqing Kunding Environmental Protection Technology, Co. Ltd., Chongqing 400044, China
3 State Key Laboratory of Power Transmission Equipments and System Security and New Technology, Chongqing University, Chongqing 400044, China

E-mails: fgao@cqu.edu.cn (F.G.), huangzhengyong@cqu.edu.cn (Z.H.), hrli@cqu.edu.cn (H.L.)

Supplementary material

Figures and Tables

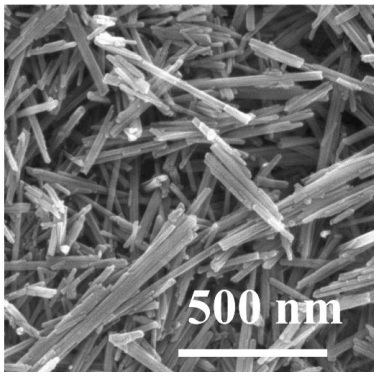

Fig. S1 SEM image of MnO_2 nanorods.

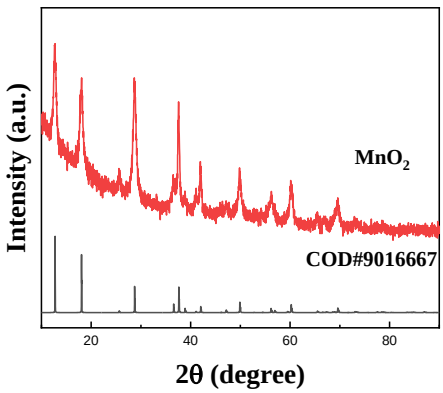

Fig. S2 The XRD pattern of MnO_2 nanorods.

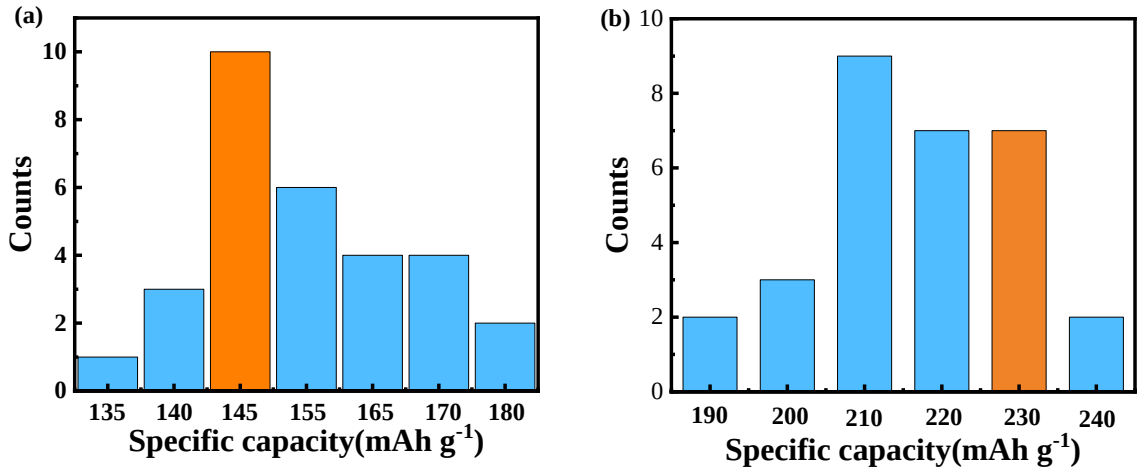

Fig. S3 Specific capacities of 30 Zn||MnO_2 full cells with different electrolytes showing a narrow distribution: **(a)** $ZnSO_4$; **(b)** 2.0 wt.% PTS/$ZnSO_4$.

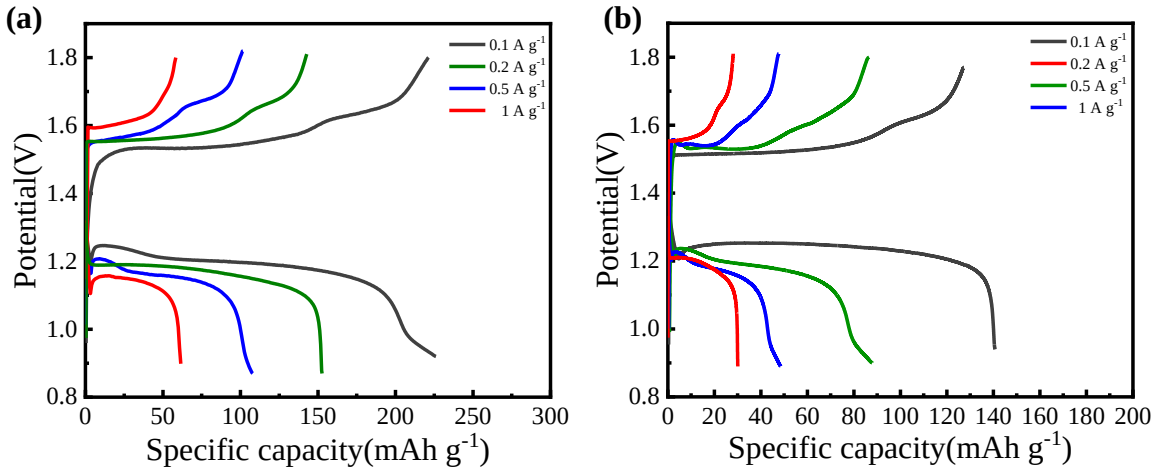

Fig. S4 Charge/discharge profiles of full Zn||MnO_2 cells in **(a)** the PTS/$ZnSO_4$ electrolyte and **(b)** the $ZnSO_4$ electrolyte.

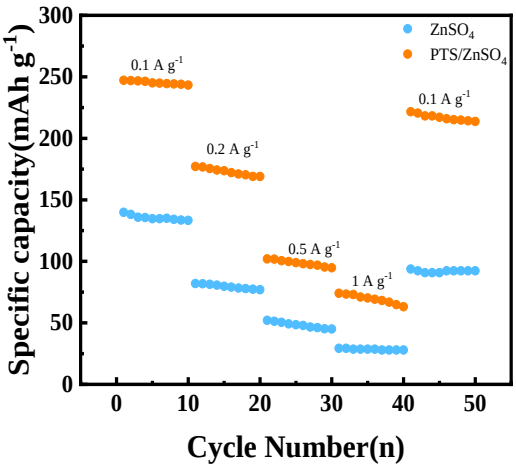

Fig. S5 Rate performance of Zn||MnO_2 full cells by using the PTS/$ZnSO_4$ and $ZnSO_4$ electrolytes.

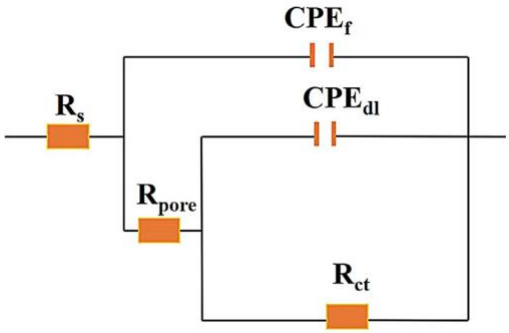

Fig. S6 Equivalent circuits for the EIS plot.

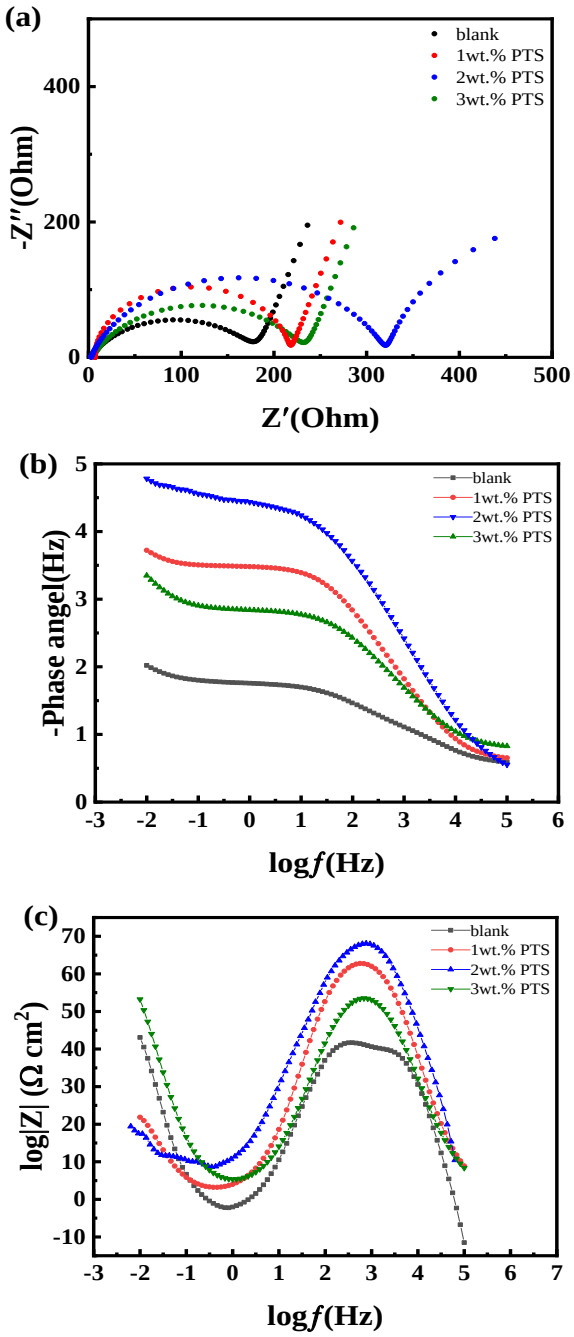

Fig. S7 (a) Nyquist plots and **(b)(c)** Bode plots for Zn||MnO_2 cells in different electrolytes.

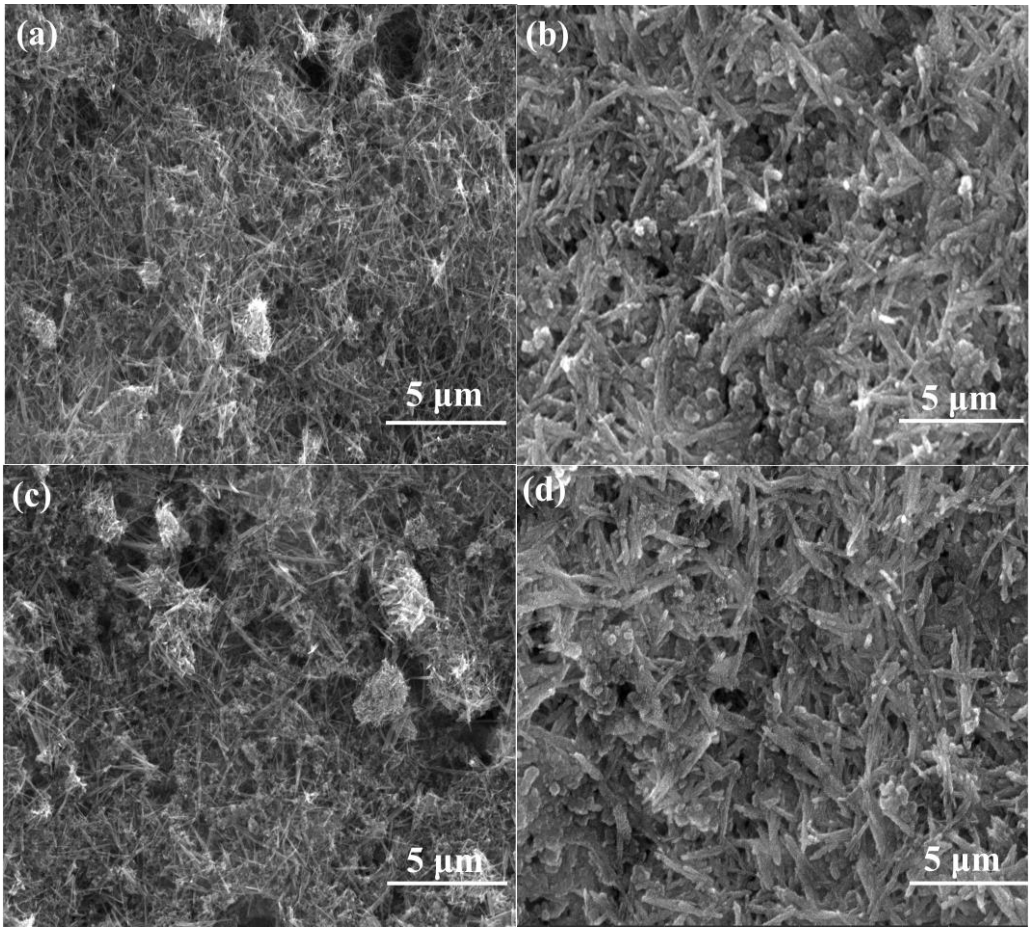

Fig. S8 SEM images of the MnO_2 cathode in Zn||MnO_2 full cells based on the $ZnSO_4$ electrolyte at 0.2 $A \cdot g^{-1}$: **(a)** before the cycle; **(b)** after 100 cycles. SEM images of the MnO_2 cathode in Zn||MnO_2 full cells based on the PTS/$ZnSO_4$ electrolyte at 0.2 $A \cdot g^{-1}$: **(c)** before the cycle; **(d)** after 100 cycles.

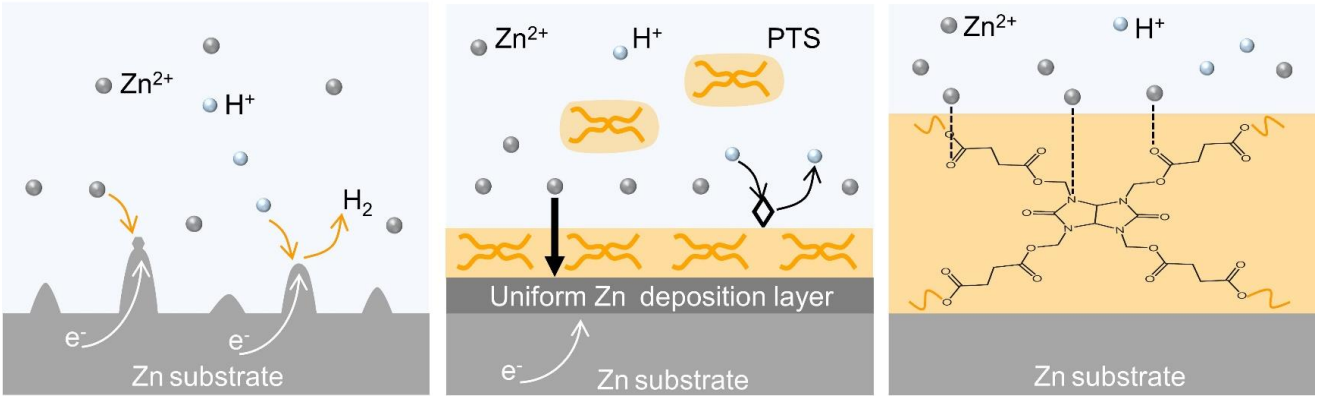

Fig. S9 Schematic diagrams for the deposition of Zn in the PTS/$ZnSO_4$ and $ZnSO_4$ electrolytes.

Table S1 EIS parameters of Zn||MnO_2 cells in different electrolytes at 298 K

Electrolyte	$R_{pore}/(\Omega \cdot cm^2)$	$R_{ct}/(\Omega \cdot cm^2)$	$R_p/(\Omega \cdot cm^2)$
$ZnSO_4$	1.881	180.8	182.681
1 wt.% PTS/$ZnSO_4$	3.021	209.8	212.821
2 wt.% PTS/$ZnSO_4$	4.541	230.3	234.841
3 wt.% PTS/$ZnSO_4$	2.767	319.8	322.567

Table S2 The performance comparison of this PTS additive strategy with previous studies in aqueous electrolytes

Main material	Current density/(mA·cm^{-2})	Areal capacity/(mA·h·cm^{-2})	Cycle time/h	Ref.
2 mol·L^{-1} $ZnSO_4$ + 2 wt.% PTS	1	1	2400	this work
	10	1	300	
	5	2	570	
1 mol·L^{-1} $ZnSO_4$ +10 mmol·L^{-1} glucose	1	1	2000	[S1]
1 mol·L^{-1} $ZnSO_4$ + 4 mol·L^{-1} EMImCl	1	1	500	[S2]
1 mol·L^{-1} $Zn(TFSI)_2$ + 0.2 wt.% PEO	1	1	1200	[S3]
2 mol·L^{-1} $ZnSO_4$ + 40% EG	2	1	140	[S4]
2 mol·L^{-1} $ZnSO_4$ + 10 m mol·L^{-1} KPF6	2	4	1200	[S5]
Zn/CNT	2	2	200	[S6]
	5	2.5	110	
MXene/ZnS	1	1	1100	[S7]
	10	1	180	
Functional supramolecules	5	3	250	[S8]

Table S3 De-convolution parameters of Zn $2p_{3/2}$ XPS spectrum peaks obtained from the pristine Zn and Zn anodes after 20 cycles in symmetric Zn||Zn cells with the PTS/$ZnSO_4$ electrolyte

Sample	Chemistry state	Binging energy/eV	FWHM/eV
Zn-bare	Zn(I)	1045.43	2.53
	Zn(II)	1022.42	2.54
Zn-PTS	Zn(I)	1045.1	2.37
	Zn(II)	1022.1	1.93

Table S4 De-convolution parameters of C 1s XPS spectrum peaks obtained from the pristine Zn and Zn anodes after 20 cycles in symmetric Zn||Zn cells with the PTS/$ZnSO_4$ electrolyte

Sample	Chemistry state	Binging energy/eV	FWHM/eV
Zn-bare	C−C	284.80	1.1
	C−O−C	285.15	1.28
	O−C=O	288.51	1.19
Zn-PTS	C−C	284.70	1.10
	C−N	287.66	1.13
	O−C=O	288.61	1.16

Table S5 De-convolution parameters of O 1s XPS spectrum peaks obtained from the pristine Zn and Zn anodes after 20 cycles in symmetric Zn||Zn cells with the PTS/$ZnSO_4$ electrolyte

Sample	Chemistry state	Binging energy/eV	FWHM/eV
Zn-bare	ZnO/Zn_2O	531.44	1.67
	O−C=O	532.00	1.40
Zn-PTS	ZnO/Zn_2O	531.7	1.45
	C=O/C−O	532.47	1.25

Table S6 De-convolution parameters of N 1s XPS spectrum peaks obtained from the pristine Zn and Zn anodes after 20 cycles in symmetric Zn||Zn cells with the PTS/$ZnSO_4$ electrolyte

Sample	Chemistry state	Binging energy/eV	FWHM/eV
Zn-PTS	Zn−N	397.2	1.01
	N=C	400.22	1.21

References

[S1] Liu T, Hong J, Wang J, et al. Uniform distribution of zinc ions achieved by functional supramolecules for stable zinc metal anode with long cycling lifespan. Energy Storage Materials, 2022, 45: 1074–1083

[S2] Sun P, Ma L, Zhou W, et al. Simultaneous regulation on solvation shell and electrode interface for dendrite-free Zn ion batteries achieved by a low-cost glucose additive. Angewandte Chemie-International Edition, 2021, 60(33): 18247–18255

[S3] Zhang Q, Ma Y, Lu Y, et al. Designing anion-type water-free Zn^{2+} solvation structure for robust Zn metal anode. Angewandte Chemie-International Edition, 2021, 60(43): 23357–23364

[S4] Yan M, Xu C, Sun Y, et al. Manipulating Zn anode reactions through salt anion involving hydrogen bonding network in aqueous electrolytes with PEO additive. Nano Energy, 2021, 82: 105739

[S5] Chang N, Li T, Li R, et al. An aqueous hybrid electrolyte for low-temperature zinc-based energy storage devices. Energy & Environmental Science, 2020, 13: 3527–3535

[S6] Chu Y, Zhang S, Wu S, et al. *In situ* built interphase with high interface energy and fast kinetics for high performance Zn metal anodes. Energy & Environmental Science, 2021, 14(6): 3609–3620

[S7] Zeng Y, Zhang X, Qin R, et al. Dendrite-free zinc deposition induced by multifunctional cnt frameworks for stable flexible zn-ion batteries. Advanced Materials, 2019, 31(36): e1903675

[S8] An Y, Tian Y, Liu C, et al. Rational design of sulfur-doped three-dimensional Ti3C2Tx MXene/ZnS heterostructure as multifunctional protective layer for dendrite-free zinc-ion batteries. ACS Nano, 2021, 15(9): 15259–15273

NMR and FT-IR spectra of the compounds

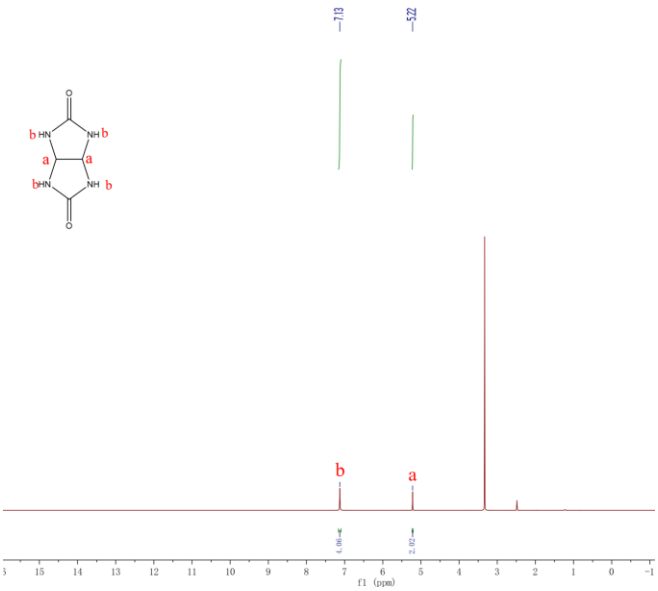

^{1}H-NMR (DMSO-d_6) spectrum of glycoluril

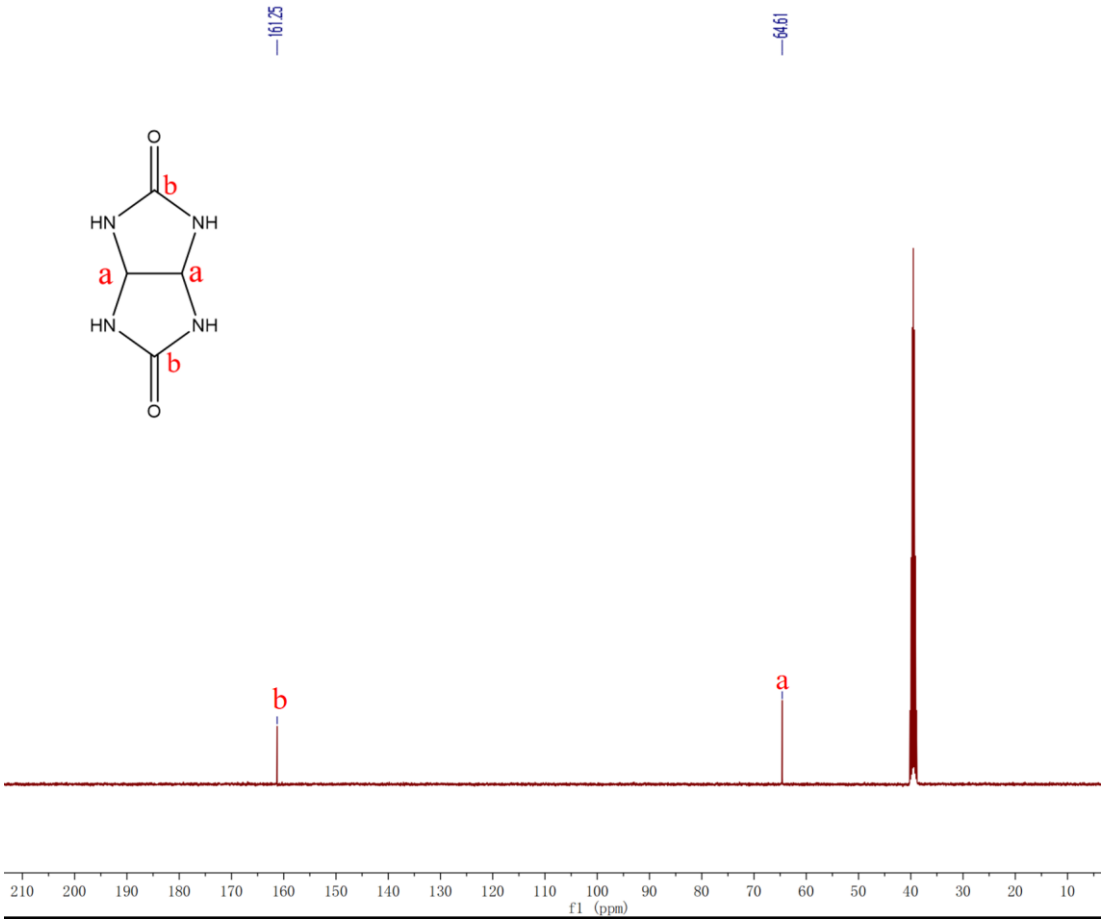

^{13}C-NMR (DMSO-d_6) spectrum of glycoluril

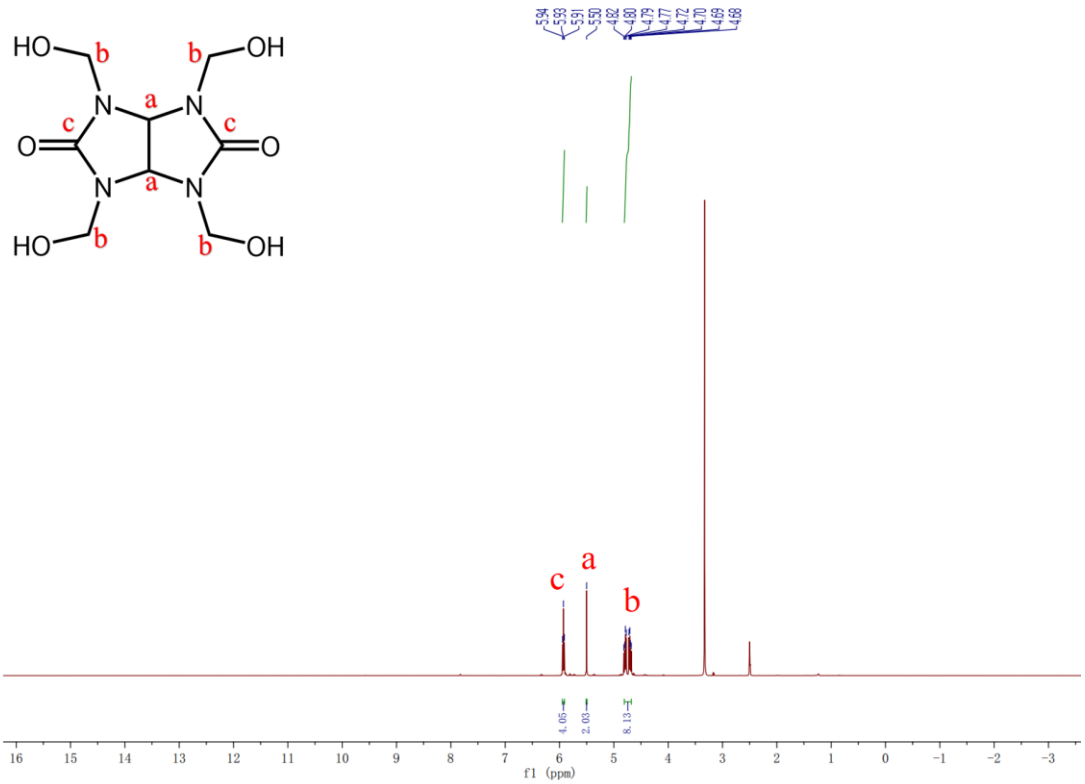

^{1}H-NMR (DMSO-d_6) spectrum of TA

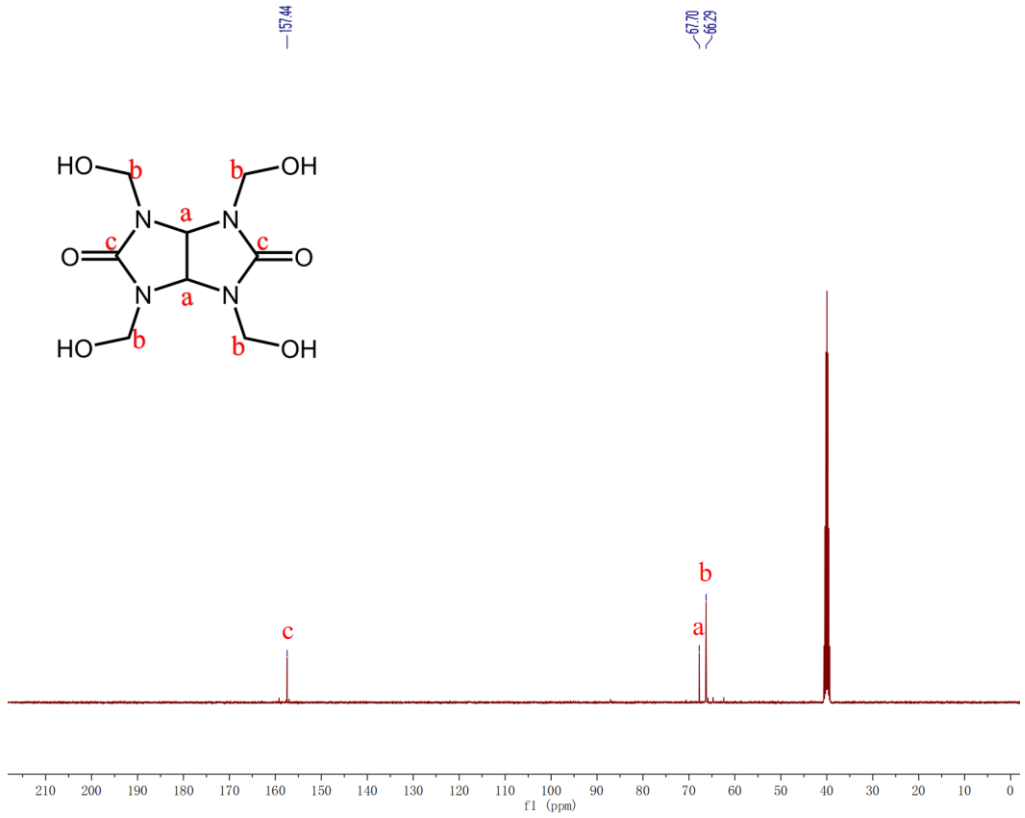

^{13}C-NMR (DMSO-d_6) spectrum of TA

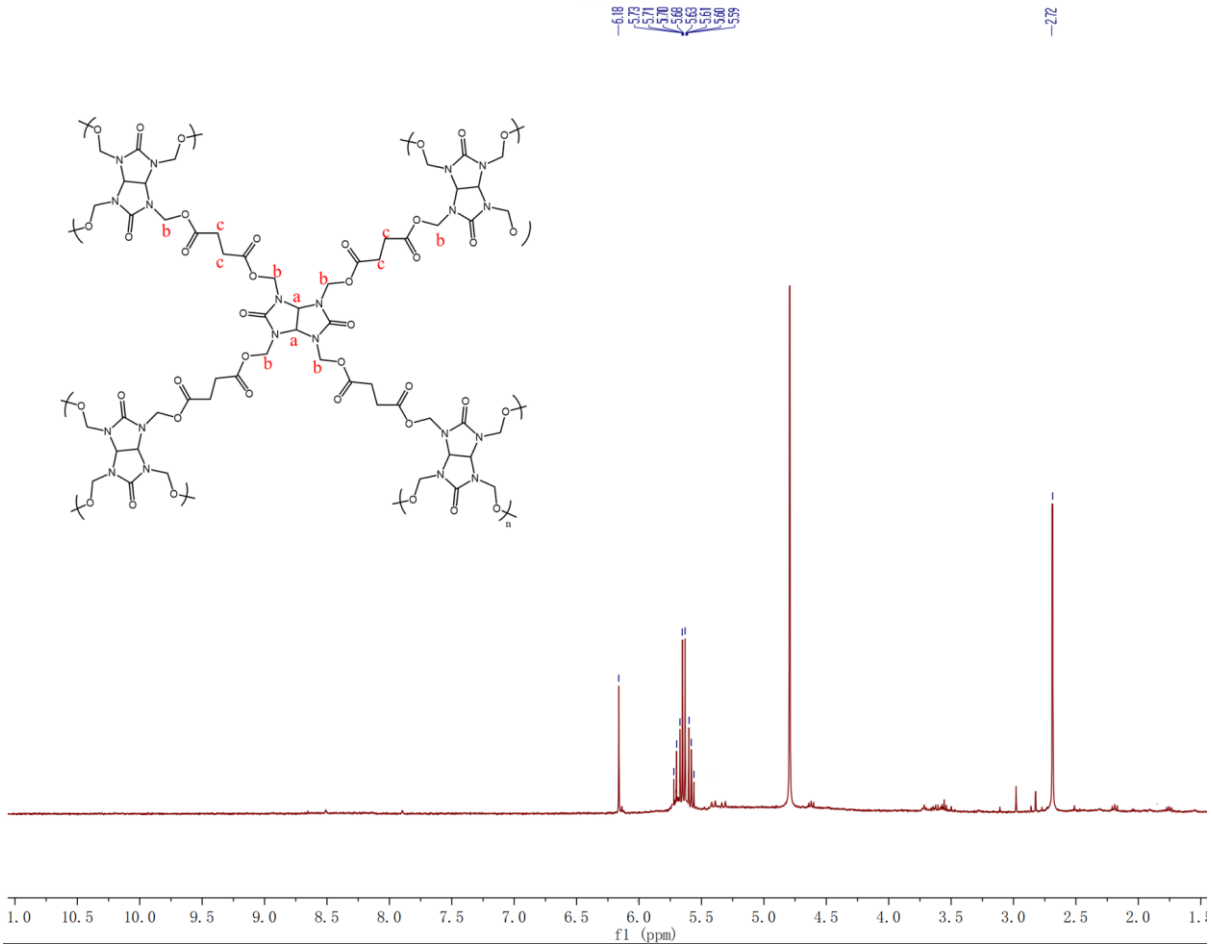

^{1}H-NMR (D_2O-d_6) spectrum of PTS

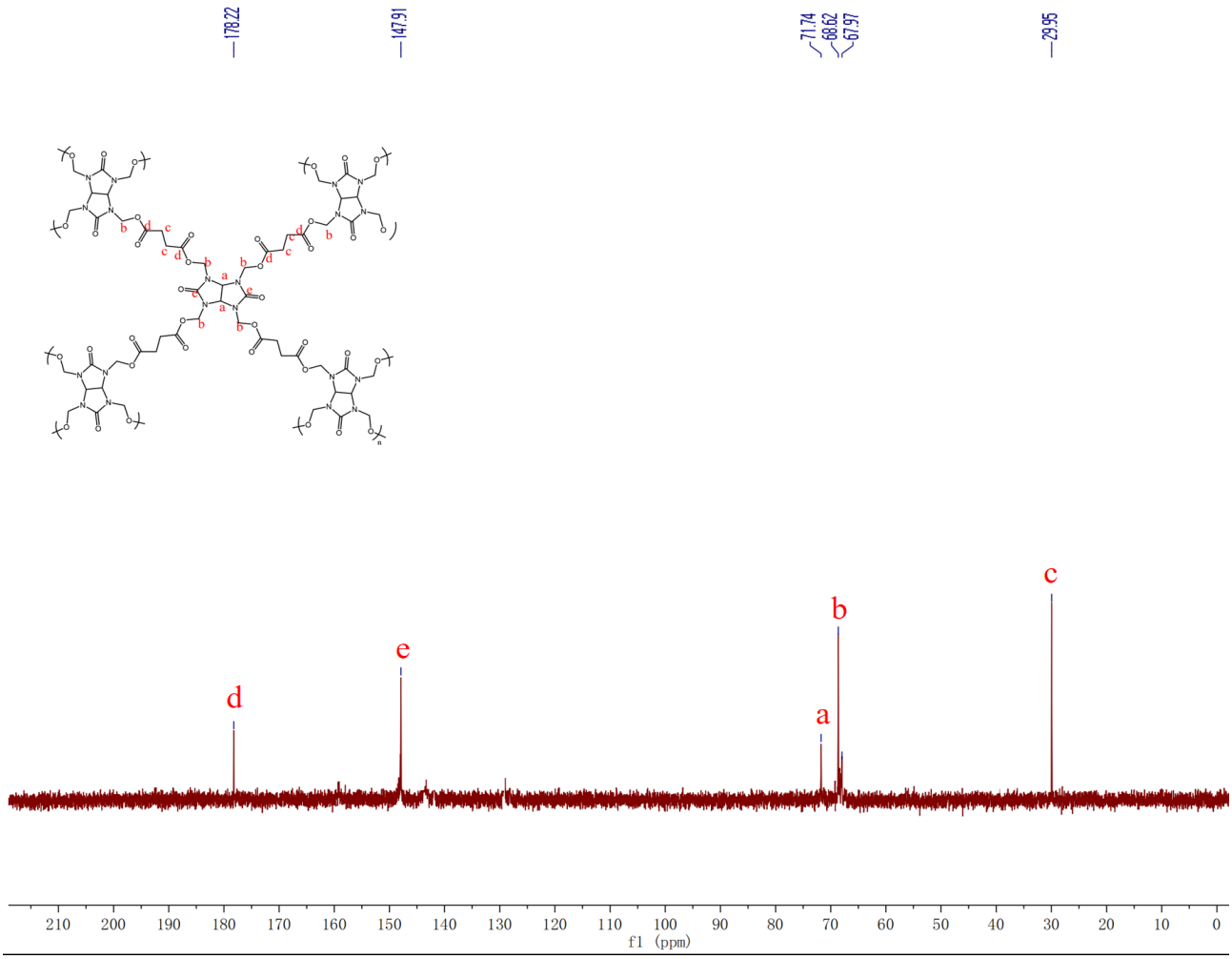

^{13}C-NMR (D_2O-d_6) spectrum of PTS

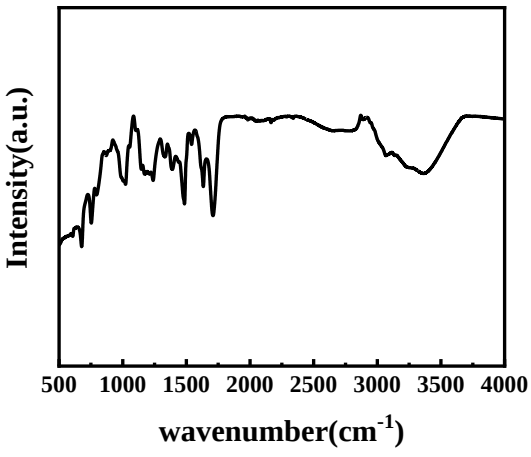

FT-IR spectrum of the PTS